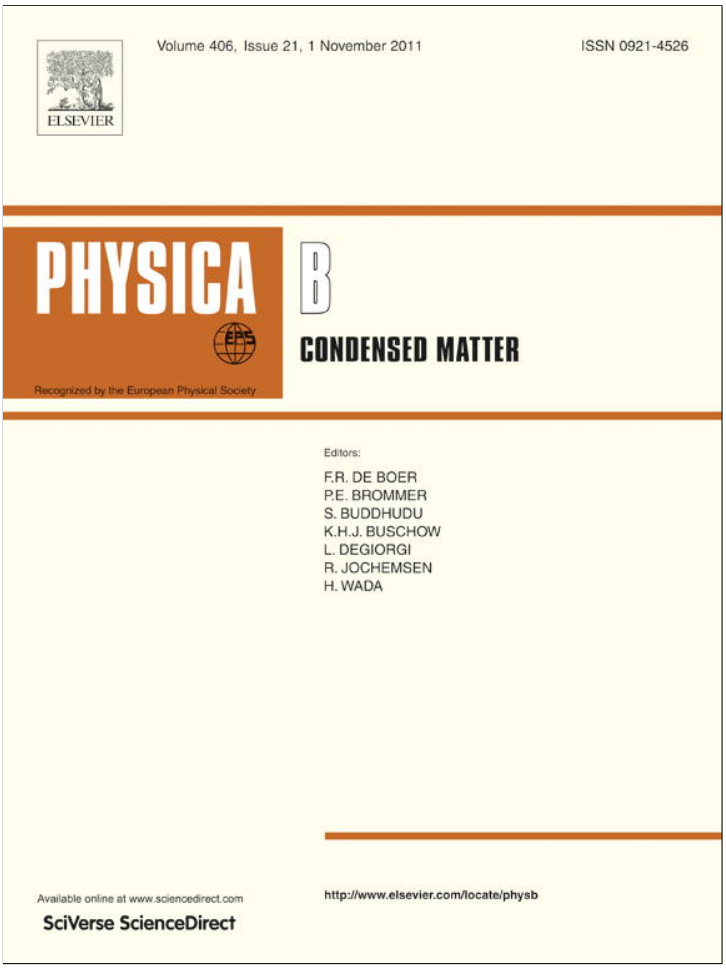

Physica B 406 (2011) 4109–4114

Contents lists available at ScienceDirect

Physica B

journal homepage: www.elsevier.com/locate/physb

A neural networks based model of inverse hysteresis

Lianwei Ma [a], Yonghong Tan [b,*], Yu Shen [c]

[a] Department of Intelligent Architecture Electrical Technology, Zhejiang University of Science & Technology, Hangzhou 310023, China
[b] College of Information, Mechanical and Electrical Engineering, Shanghai Normal University, Shanghai 200234, China
[c] Department of Applied Physics, Zhejiang University of Science and Technology, Hangzhou 310023, China

ARTICLE INFO

Article history:
Received 16 October 2008
Received in revised form
30 July 2011
Accepted 31 July 2011
Available online 3 August 2011

Keywords:
Inverse hysteresis
Elementary inverse hysteresis operator
Continuous transformation
Neural network

ABSTRACT

A novel and simple approach based on transformation using neural networks is proposed in this paper to model the inverse behavior of hysteresis. In this approach, a continuous transformation is used to construct an elementary inverse hysteresis operator (EIHO), which can extract the change tendency of inverse hysteresis. Then based on the EIHO, an expanded input space is constructed to transform the multi-valued mapping of inverse hysteresis into a one-to-one mapping. Based on the constructed expanded input space, a neural network is employed to approximate the inverse hysteresis. Both experiment and simulation are implemented to validate the effectiveness of the proposed approach. These results indicate that the proposed approach has derived satisfactory modeling performance.

1. Introduction

It is well known that hysteresis is a non-differentiable nonlinearity with multi-valued mapping. Usually, hysteresis exists in physical systems such as magnetic suspensions, bearings, piezoelectric actuators, etc. The presence of hysteresis often severely limits system performance, giving rise to undesirable inaccuracy, oscillations, or even leading to instability for closed-loop control systems.

The existent compensation methods for hysteresis usually depend upon the inverse models based technique. However, the inverse model based compensation often requires accurate inverse model for hysteresis. Several inverse hysteresis models have been proposed in past several years, e.g. Kuhnen [1] constructed inverse hysteresis model based on modified PI operator. Hu and Ben Mrad [2] proposed a discrete-time compensation algorithm for hysteresis based on first-order reversal functions. Tan and Bennani [3] developed Preisach-type inverse hysteresis model using field-programmable gate arrays.

Note that neural networks have many advantages in nonlinearity identification, such as: self-learning, associative memory, high speed sought optimization solution, etc. In past decade, neural networks (NN) have been successfully used in many fields, including the modeling of hysteresis, e.g. Zhao et al. [4], Zhao and Tan [5], Ma et al. [6] and Dong et al. [7] model hysteresis using neural networks. However, neural networks based method has been seldom found in the literatures on the inverse hysteresis model so far. Zao et al. proposed a neural network based inverse hysteresis model in Ref. [8]. However, the precision of the inverse model may not be guaranteed when it is used to model backlash inverse hysteresis. Thus, looking for a method to model the inverse hysteresis with multi-loop using neural networks is a real challenge.

It has been proven that traditional approach of neural networks cannot approximate the nonlinear with multi-value mapping. An elementary inverse hysteresis operator (EIHO) is constructed using continuous transformation approach in this paper. The EIHO extracts the basic change trend of inverse hysteresis. Then based on the EIHO, an expanded input space is constructed. Based on the constructed expanded input space, a neural network is employed to approximate the inverse hysteresis. The inverse hysteresis model is tested with a set of real data and simulation.

2. Construction of the elementary inverse hysteresis operator (EIHO)

The elementary inverse hysteresis operator (EIHO) adopts the continuous transformation approach to build one-to-one mapping between the input and the output of hysteresis. The basic idea is that when an extremum of input occurs, a new coordinate system is constructed. Then in the new coordinate system, a motion point moves along a regular curve, such as inversion of a monotone conic, and produces a branch of main or minor loops. By continuously transforming, an arbitrary number of inverse

* Corresponding author.
E-mail address: tanyongh@yahoo.com.cn (Y. Tan).

0921-4526/$ - see front matter © 2011 Elsevier B.V. All rights reserved.
doi:10.1016/j.physb.2011.07.061

hysteresis minor loops can be obtained so that an elementary inverse hysteresis operator (EIHO) can be constructed.

A plane of Cartesian coordinate system (e.g., point o, x–y, Fig. 1) that is called major coordinate system is constructed. When an input extremum occurs, another coordinate system (e.g., point i, x_i–y_i, Fig. 1) is constructed to form the corresponding ith minor coordinate system. Let the motion point move along a monotone curve under the minor coordinate to produce a branch of minor loops, so does every extremum point. The monotone curve is used to replace each branch of the minor and the major loops. The equation of coordinate transformation is described below [9]

$$\begin{bmatrix} x(t) \\ y(t) \end{bmatrix} = \begin{bmatrix} \cos\theta_i & -\sin\theta_i \\ \sin\theta_i & \cos\theta_i \end{bmatrix} \begin{bmatrix} x'(t) \\ y'(t) \end{bmatrix} + \begin{bmatrix} x_i(t) \\ y_i(t) \end{bmatrix} \tag{1}$$

where $x_i(t)$ and $y_i(t)$ are the ith input extremum and the corresponding calculated output, respectively. It is also the original point of the ith minor coordinate system. $x'(t)$ and $y'(t)$ are the input and the calculated output under the ith minor coordinate system. On the other hand, $x(t)$ and $y(t)$ are the actual input and the calculated output under the major coordinate system. θ_i is the transformation angle of the ith minor coordinate system to the major coordinate system. Notice that the above calculated output values are computed via suitably selected curve equations. Here it is supposed to have the following assumption to obtain this conclusion:

Assumption 1. Suppose the input is a smoothly periodical signal, and there are no continuously uniform maxima and minima pairs in a cycle.

Fig. 2 shows the corresponding situation excluded by Assumption 1. The mapped inverse hysteresis curve of the two continuously uniform maxima and minima pairs (bounded by dotted lines) are completely superposed into two minor loops. In this situation, it cannot be found that the relation between the input and output is a one-to-one mapping.

The inversion of monotone conic is adopted as the monotone curve in this paper. Therefore, the proposed EIHO $f(x)$ is defined as

$$f(x) = \begin{cases} f(x_e) + a[x - x_e]^{1/2} & \dot{x} > 0, \\ f(x_e) - a[x_e - x]^{1/2} & \dot{x} < 0. \end{cases} \tag{2}$$

where x is the current input, $f(x)$ is the current output, a ($a > 0$) is the coefficient of the inverse conic, x_e is the dominant extremum adjacent to the current input x. $f(x_e)$ is the output of the EIHO when the input is x_e.

The EIHO extracts the elementary information of inverse hysteresis, such as ascending, turning and descending. The output of the EIHO and the input of the inverse hysteresis are used as the input signals of a common neural network (NN) so that the expanded input space can be constructed. Based on the constructed expanded input space, a neural network can be used to approximate inverse hysteresis.

3. EIHO-based neural network model

A three-layer neural network with two inputs and one output is used to model inverse hysteresis. The output of the EIHO and $x(t)$ are used as the input fed to NN. The block diagram is shown in Fig. 3. The traditional approach of neural networks can only approximate the nonlinear functions with one-to-one or multi-to-one mapping [10]. In the following, it will be proved that the relation between the input space ($x(t)$, $f[x(t)]$) and the output space ($IH[x(t)]$) of NN is a continuous one-to-one mapping.

Lemma 1. *Let $x(t) \in C(R)$, where $R = \{t \mid -\infty < t < \infty\}$ and $C(R)$ are the sets of continuous functions on R. For the different time instants t_1 and t_2 ($t_1 \neq t_2$), $x(t_1) = x(t_2)$ but it leads to $f[x(t_1)] \neq f[x(t_2)]$.*

Proof. Considering the segment $x(t)$ decreases monotonically, Eq. (2) becomes

$$f(x) = f_{de}(x) = f(x_e) - a[x_e - x]^{1/2} \quad a > 0 \tag{3}$$

where $f_{de}(x)$ is the decreasing segment of the function, x_e is the maximum extremum of the input, whilst

$$f(x) = f_{in}(x) = f(x_e) + a[x - x_e]^{1/2} \quad a > 0 \tag{4}$$

denotes the increasing segment of the function. In this case, x_e is the minimum extremum of the input. Since

$$\frac{df_{in}(x)}{dx} = \frac{a}{2\sqrt{x - x_e}} > 0 \tag{5}$$

and

$$\frac{df_{de}(x)}{dx} = \frac{a}{2\sqrt{x_e - x}} > 0 \tag{6}$$

Therefore, $f_{in}(x)$ and $f_{de}(x)$ are monotonic.

It is noted that $t_1 \neq t_2$ and $x(t_1) = x(t_2)$ in Fig. 4. x_{e1} and x_{e2} are, respectively, the dominant extrema of $x(t_1)$ and $x(t_2)$. According to Eq. (3)

$$f[x(t_1)] = f(x_{e1}) - a_1[x_{e1} - x(t_1)]^{1/2} \tag{7}$$

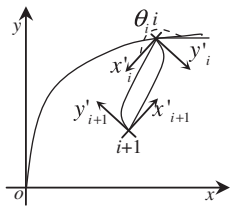

Fig. 1. Coordinate transformation.

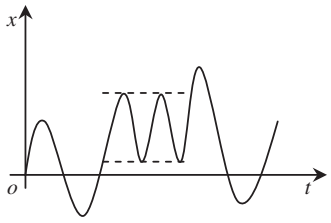

Fig. 2. Excluded time-varying input signal.

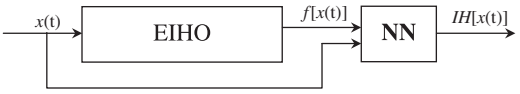

Fig. 3. EIHO-based neural network model.

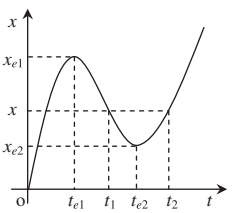

Fig. 4. Time-varying input signal.

and

$$f(x_{e2}) = f(x_{e1}) - a_1(x_{e1} - x_{e2})^{1/2} \tag{8}$$

Based on Eq. (4), it yields

$$f[x(t_2)] = f(x_{e2}) + a_2[x(t_2) - x_{e2}]^{1/2} = f(x_{e1}) - a_1(x_{e1} - x_{e2})^{1/2} + a_2[x(t_2) - x_{e2}]^{1/2} \tag{9}$$

Furthermore,

$$\begin{aligned} f[x(t_1)] - f[x(t_2)] &= f(x_{e1}) - a_1[x_{e1} - x(t_1)]^{1/2} - f(x_{e1}) \\ &\quad + a_1(x_{e1} - x_{e2})^{1/2} - a_2[x(t_2) - x_{e2}]^{1/2} \\ &= a_1(x_{e1} - x_{e2})^{1/2} - a_1[x_{e1} - x(t_1)]^{1/2} - a_2[x(t_2) - x_{e2}]^{1/2} \end{aligned} \tag{10}$$

Since $x(t_1) = x(t_2)$, Eq. (10) becomes

$$f[x(t_1)] - f[x(t_2)] = a_1(x_{e1} - x_{e2})^{1/2} - a_1[x_{e1} - x(t_1)]^{1/2} - a_2[x(t_1) - x_{e2}]^{1/2} \neq 0 \tag{11}$$

Thus, for two particular time instants t_1 and t_2 ($t_1 \neq t_2$), even though $x(t_1) = x(t_2)$, $f[x(t_1)] \neq f[x(t_2)]$ since their dominant extrema are different.

Remark 1. $IH[\cdot]$ is defined as the output of inverse hysteresis. When $f(x)$ and $IH[\cdot]$ are fed with the same input $x(t)$, the curve of $f[x(t)]$ exhibits similarity to that of $IH[\cdot]$ such as ascending, turning and descending. (Fig. 5).

In the following, an example is provided to illustrate this similarity. It is known that the sum of a number of backlash operators can be used to construct a backlash hysteresis. Suppose a backlash hysteresis is constructed by 10 backlash operators with the values of the deadband width evenly distributed within (0.5, 5). The input fed into the hysteresis is $x(t) = 2\sin(3t) + 3\sin(0.5t)$. The output and input of the backlash hysteresis are, respectively, used as the input and output of the inverse backlash hysteresis. The plot of the proposed EIHO (solid) and the corresponding inverse hysteresis curve (dashed) are shown in Fig. 6. It can be seen that the proposed EIHO can extract the main feature of the inverse hysteresis if it is fed with the same input as that of the inverse hysteresis.

Remark 2. Since $x(t_1) = x(t_2)$, where $x(t_1)$ and $x(t_2)$ are not the extrema, and $f[x(t_1)] \neq f[x(t_2)]$, then the coordinate $(x(t), f[x(t)])$ is uniquely corresponding to inverse hysteresis $IH[x(t)]$.

Lemma 2. *If there exist two time instants t_1 and t_2, also $t_1 \neq t_2$, such that $f[x(t_1)] - f[x(t_2)] \to 0$, then $x(t_1) - x(t_2) \to 0$.*

Proof. Considering

$$\frac{f_{in}[x(t_1)] - f_{in}[x(t_2)]}{x(t_1) - x(t_2)} = k, \quad k \in (0, +\infty) \tag{12}$$

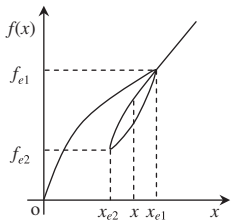

Fig. 5. Input signal–output signal of EIHO.

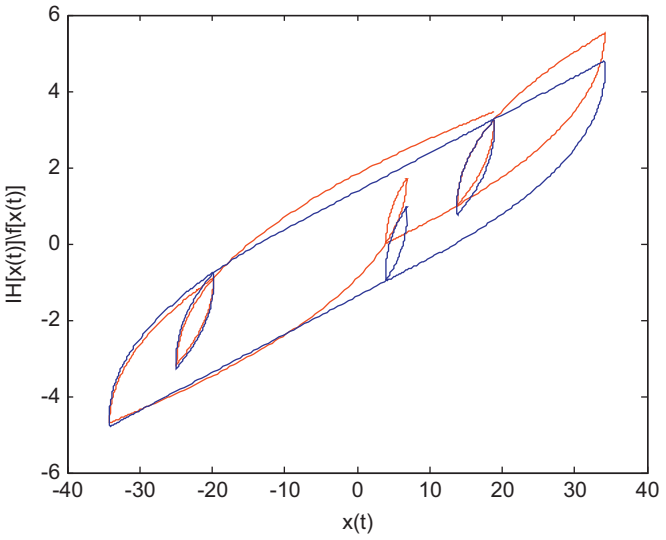

Fig. 6. Comparison between the plot of EIHO (solid, $a_i = 1$) and inverse hysteresis curve (dashed).

Then

$$x(t_1) - x(t_2) = \frac{f_{in}[x(t_1)] - f_{in}[x(t_2)]}{k} \tag{13}$$

It is clear that if $f_{in}[x(t_1)] - f_{in}[x(t_2)] \to 0$, then $x(t_1) - x(t_2) \to 0$. Similarly, it can be obtained that if $f_{de}[x(t_1)] - f_{de}[x(t_2)] \to 0$, then $x(t_1) - x(t_2) \to 0$.

Theorem 1. *For any inverse hysteresis, there exists a continuous one-to-one mapping $\Gamma: R^2 \to R$, such that $IH[x(t)] = \Gamma(x(t), f[x(t)])$.*

Proof. First, it is proved that Γ is a one-to-one mapping.

In terms of Lemma 1, if there exist two different time instant t_1 and t_2, then

$$(x(t_1), f[x(t_1)]) \neq (x(t_2), f[x(t_2)]) \tag{14}$$

Therefore, the coordinate $(x(t), f[x(t)])$ is uniquely corresponding to inverse hysteresis $IH[x(t)]$, that is to say, Γ is a one-to-one mapping.

Next, it will be proved that Γ is a continuous mapping.

In terms of Ref. [11],

$$x(t_1) - x(t_2) \to 0 \Rightarrow f[x(t_1)] - f[x(t_2)] \to 0 \tag{15}$$

Then, considering Lemma 2,

$$\begin{aligned} f[x(t_1)] - f[x(t_2)] \to 0 &\Rightarrow x(t_1) - x(t_2) \to 0 \\ &\Rightarrow IH[x(t_1)] - IH[x(t_2)] \to 0 \end{aligned} \tag{16}$$

Therefore, it can be concluded that there exists a continuous one-to-one mapping $\Gamma: R^2 \to R$ such that $IH[x(t)] = \Gamma(x(t), f[x(t)])$.

Remark 3. Theorem 1 indicates that the proposed EIHO can transform the multi-valued mapping of inverse hysteresis into a continuous one-to-one mapping.

It is well known that any continuous one-to-one mapping can be approximated to arbitrary accuracy on a compact set using a three-layer neural network (NN) that contains a sufficient number of hidden layer neurons and data [12–14]. The NN consists of I input nodes, hidden layer J neurons and output layer K neurons. With all the NN weights collected into matrices $\boldsymbol{V^T}$ and $\boldsymbol{W^T}$, the NN equation with linear output activation function may be written in terms of vectors as

$$\boldsymbol{Y} = \boldsymbol{W^T}\sigma(\boldsymbol{V^T X}) \tag{17}$$

where $\boldsymbol{V^T}=[v_{ij}]^T$ and $\boldsymbol{W^T}=[w_{jk}]^T$ are the first-to-second layer interconnection weight matrix and the second-to the third layer interconnection weight matrix, respectively, where $i=1, 2,\ldots,I$; $j=1, 2,\ldots J$; $k=1, 2,\ldots,K$; $\boldsymbol{X}=[x_1, x_2,\ldots,x_I]$; $\boldsymbol{Y}=[y_1, y_2,\ldots,y_K]^T$. The scalar function $\sigma(\cdot)$ is a sigmoidal activation function of the hidden layer neurons.

4. Calculation of a_i in EIHO

Suppose that all a_i's are equal to 1 in Fig. 6. In fact, the more precise the matched EIHO is, the more accurate the approximated result is derived. The precision is not guaranteed if $a_i=1$ in each modeling procedure. Therefore, it is necessary to propose a new method to calculate a_i. The adequate real data that is used to train neural network to calculate a_i is employed for computation.

Suppose that $x(t_i)$ and $y(t_i)$ are, respectively, the ith input extremum and the corresponding output; $x(t_{i+1})$ and $y(t_{i+1})$ are, respectively, the $(i+1)$-th input extremum and the corresponding output. According to Eq. (2),

$$y(t_{i+1})=\begin{cases} y(t_i)+a_i[x(t_{i+1})-x(t_i)]^2 & \text{if } x(t_{i+1})>x(t_i) \\ y(t_i)-a_i[x(t_{i+1})-x(t_i)]^2 & \text{if } x(t_{i+1})<x(t_i) \end{cases} \tag{18}$$

Thus,

$$a_i=\begin{cases} \frac{y(t_{i+1})-y(t_i)}{[x(t_{i+1})-x(t_i)]^2} & \text{if } x(t_{i+1})>x(t_i) \\ \frac{y(t_i)-y(t_{i+1})}{[x(t_{i+1})-x(t_i)]^2} & \text{if } x(t_{i+1})<x(t_i) \end{cases} \tag{19}$$

where a_i is the parameter of ith parabola.

5. Implementation of EIHO-based NN model

In the following, two examples are presented. In these examples, the conjugate gradient algorithm with Powell–Beale restarted method is used to train the neural network, so as to improve the convergent rate and the performance of the neural model.

5.1. Experimental example

In this example, the proposed method is applied to the modeling of a set of real data measured from a piezoelectric actuator PZT-753.21C, made by PI Company. The actuator has a nominal expansion of 0–25 μm ($x(t)$) under an input voltage of 0–100 V ($IH[x(t)]$), with a 1000 Hz sampling frequency.

A three-layer feed-forward neural network is used to approximate the real data. The sigmoid function and linear function are, respectively, used as activation function in the hidden layer and output layer. Two thousand three hundred and one pairs of measured data are implemented. The proposed EIHO-based NN model is used to approximate it.

It is found that the neural network derives the best results when the number of hidden neurons becomes 152. Therefore, the architecture of neural network used in this example consists of 2 input neurons, 152 hidden neurons and 1 output neuron. After 319 epochs, the training procedure is finished. Fig. 7 illustrates the result of model validation. The MSE is 5.0360e−005. Fig. 8 shows the model validation error.

Moreover, the model based on the method given in Ref. [8] is used to approximate the real data. It is found that the network derives the best results when the number of hidden neurons becomes 82. After 520 epochs, the training procedure is finished. Fig. 9 illustrates the result of model validation. The MSE is 1.0254e−004. Fig. 10 shows the model validation error.

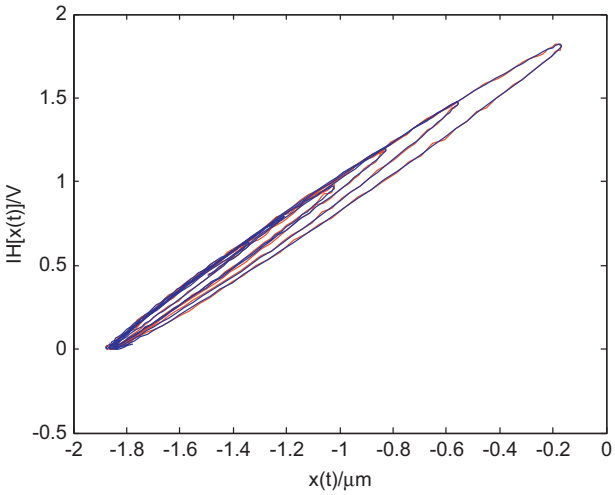

Fig. 7. Comparison between the EHIO-based NN prediction (dashed) and the real data (solid).

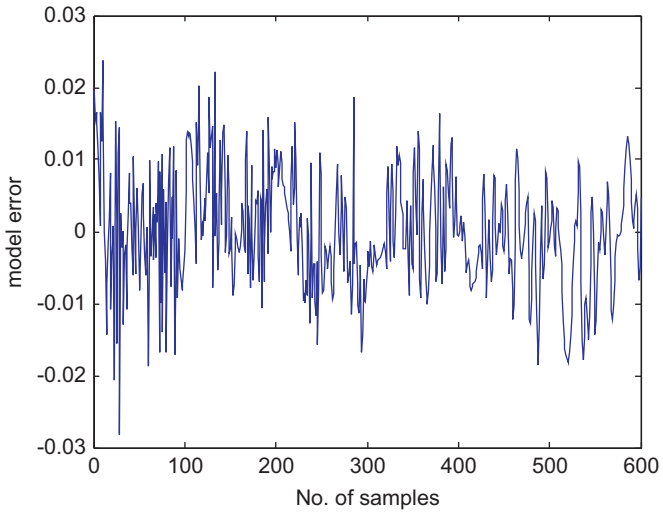

Fig. 8. EHIO-based NN model validation error for the real data.

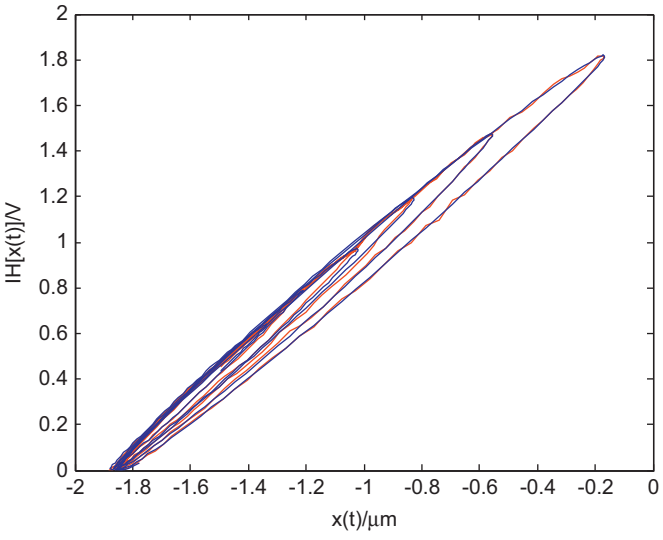

Fig. 9. Comparison between the prediction of the model based on the method given in Ref. [8] (dashed) and the real data (solid).

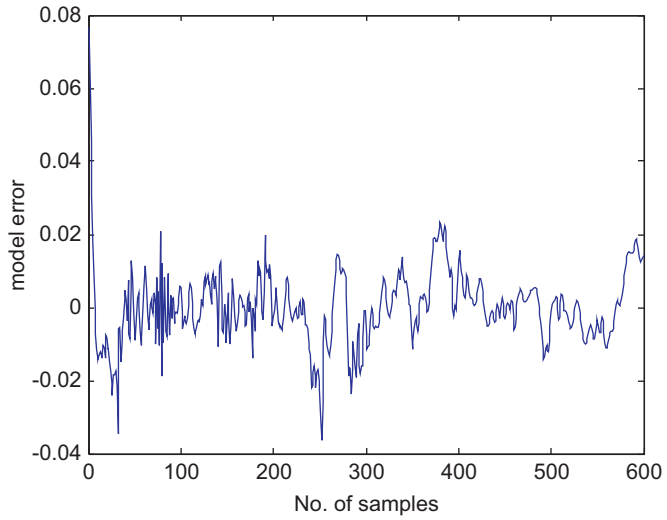

Fig. 10. Model validation error for the real data based on the method given in Ref. [8].

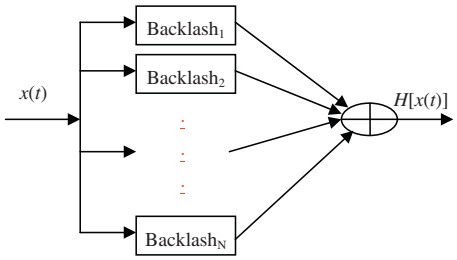

Fig. 11. Block diagram of backlash hysteresis.

By comparing the result of the proposed model with that of the model using the method given in Ref. [8], it shows that the proposed model has obtained better performance.

5.2. Simulation

It is known that the sum of a number of backlash operators can be used to construct a backlash hysteresis. The backlash operator is given by

$$\dot{y}_i = \begin{cases} \dot{x}_i(t) & \dot{x}_i > 0, y_i(t) = x_i(t) - \frac{1}{2}d_i, \\ \dot{x}_i(t) & \dot{x}_i < 0, y_i(t) = x_i(t) + \frac{1}{2}d_i, \\ 0 & \text{otherwise} \end{cases} \quad (20)$$

Thus, a backlash hysteresis is given as follows:

$$H[x(t)] = \sum_{i=1}^{N} y_i \quad (21)$$

where N is number of backlash operator, $x(t)$ and $H[x(t)]$ are input and output of the backlash hysteresis, x_i and y_i are input and output of the ith backlash operator, d_i is dead-band width of the ith backlash operator, $i=1, 2,\ldots,N$, where N is a positive integer. The constructed backlash hysteresis is shown as Fig. 11.

In this example, the backlash hysteresis consists of 15 backlash operators. The dead-band width values evenly distributed in [1/6, 15/6]. All the initial outputs are set to zero. The input is $x(t)=4\sin(0.5t)+2\sin(3t)$. The output and input of the backlash hysteresis are, respectively, used as the input and output of the inverse backlash hysteresis.

A three-layer feed-forward neural network is used to approximate the inverse backlash hysteresis. The sigmoid function and linear function are, respectively, used as activation function in the hidden layer and output layer.

It is found that the neural network derives the best results when the number of hidden neurons becomes 168. Therefore, the architecture of neural network used in this example consists of 2 input neurons, 168 hidden neurons and 1 output neuron. After 1504 epochs, the training procedure is finished. Fig. 12 illustrates the result of model validation. The MSE is 0.001737. Fig. 13 shows the corresponding model validation error.

In addition, the model based on the method given in Ref. [8] is used to approximate the inverse backlash hysteresis for comparison as well. It is found that the network derives the best results when the number of hidden neurons becomes 169. After 1624 epochs, the training procedure is finished. Fig. 14 illustrates the result of model validation. The MSE is 0.003867. Fig. 15 shows the model validation error.

On comparing the result of the proposed model validation with that of the model based on the method given in Ref. [8], it

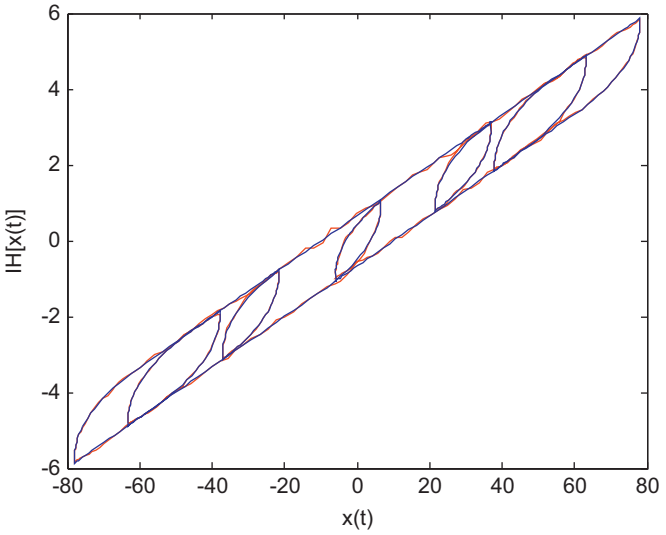

Fig. 12. Comparison between the EHIO-based NN prediction (solid) and inverse hysteresis output (dashed).

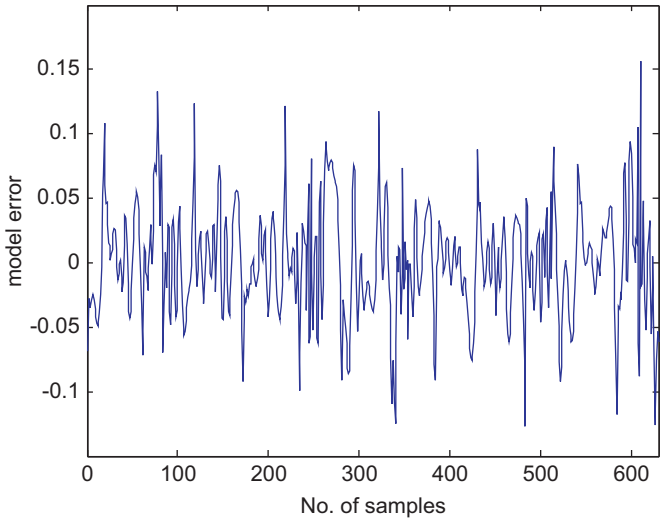

Fig. 13. EHIO-based NN model validation error for the inverse backlash hysteresis.

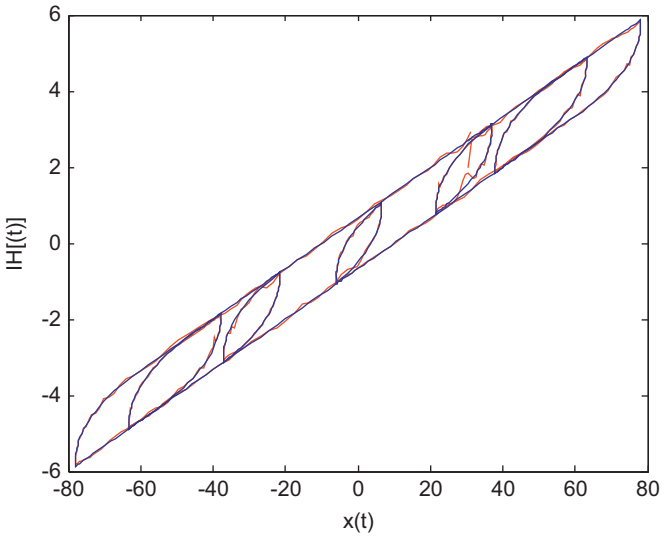

Fig. 14. Comparison between the prediction of the model based on the method given in Ref. [8] (solid) and inverse hysteresis output (dashed).

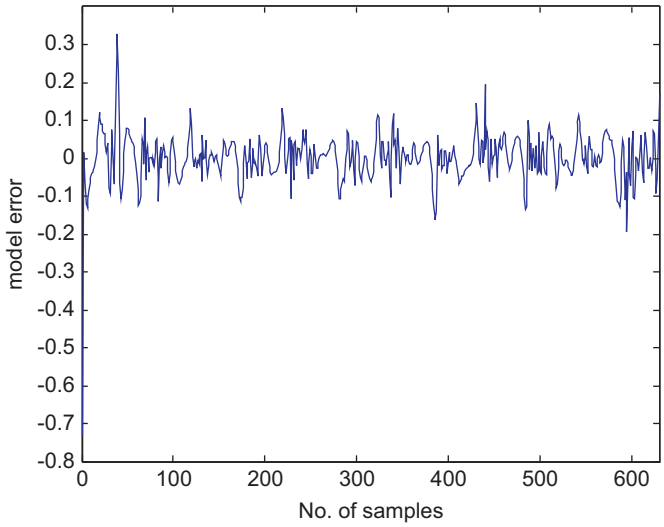

Fig. 15. Model validation error for the inverse backlash hysteresis based on the method given in Ref. [8].

illustrates that the proposed model can approximate the inverse backlash hysteresis better than the model based on the method given in Ref. [8].

The above-stated examples show that the proposed method is promising for modeling inverse hysteresis.

6. Conclusion

In this paper, an EIHO-based NN inverse hysteresis model is proposed. The EIHO constructs a one-to-one mapping relation between the input space and the output space of inverse hysteresis, and therefore, theoretically the EIHO-based NN model can approximate any inverse hysteresis whose input signals satisfy Assumption 1. Both experimental results and simulation validate the effectiveness of the proposed modeling method.

Acknowledgments

This work is partially supported by Zhejiang Science Foundation (ZJSF) (Grant no.: Y1110508), the Leading Academic Discipline Project of Shanghai Normal University (Grant no.: DZL811), the Innovation Program of Shanghai Municipal Education Commission (Grant nos.:09ZZ141 and 11YZ92), the Advanced Research Grant of Shanghai Normal University (Grant nos.: DYL201005, DYL201006 and DRL904), the National Science Foundation of China (NSFC Grant no.:60971004), the Natural Science Foundation of Shanghai (Grant nos.: 09ZR1423400 and 10ZR1422400) and the Science and Technology Commission of Shanghai Municipality (Grants nos.: 09220503000 and 10JC1412200).

References

[1] K. Kuhnen, Eur. J. Control 9 (4) (2003) 407.
[2] H. Hu, R. Ben Mrad, Mech. Syst. Signal Process. 18 (1) (2004) 169.
[3] Xiaobo Tan, Omar Bennani, Fast inverse compensation of Preisach-type hysteresis operators using field-programmable gate arrays, in: Proceedings of the American Control Conference, Seattle, Washington, USA, 2008.
[4] Tong Zhao, Yonghong Tan, Xianwen Zeng, Sensors Actuators A: Phys. 119 (1) (2005) 254.
[5] Xinlong Zhao, Yonghong Tan, Sensors Actuators A: Phys. 126 (2) (2006) 306.
[6] Lianwei Ma, Yonghong Tan, Ya Chu, Sensors Actuators A: Phys. 141 (1) (2008) 6.
[7] Ruili Dong, Yonghong Tan, Hui Chen, Yangqiu Xie, Sensors Actuators A: Phys. 143 (3) (2008) 370.
[8] Xinlong Zhao, Yonghong Tan, Jianping Dong, J. Shanghai Jiaotong Univ. 41 (1) (2007) 104.
[9] C. Wexler, Analytic Geometry: A Vector Approach, Addison-Wesley Publishing Company Inc, 1967.
[10] J.D. Wei, C.T. Sun, IEEE Trans. Syst. Man Cybern. 30 (4) (2000) 601.
[11] R.B. Gorbert, Control of Hysteretic System with Preisach Representation, Ph.D. Thesis of University of Waterloo, Ontario, Canada, 1997.
[12] Neural Networks Toolbox For Use with Matlab, The Mathworks Inc., 1999.
[13] G. Cybenko, Math. Control Signals Syst. 2 (4) (1989) 303.
[14] K. Funahashi, Neural Networks 2 (1989) 183.